Microbiology (2004), **150**, 3229–3241 DOI 10.1099/mic.0.27352-0

Saccharomyces cerevisiae Bni4p directs the formation of the chitin ring and also participates in the correct assembly of the septum structure

M. Sanz, F. Castrejón, A. Durán and C. Roncero

Instituto de Microbiología Bioquímica, Consejo Superior de Investigaciones Científicas/ Universidad de Salamanca and Departamento de Microbiología y Genética, Universidad de Salamanca. 37007 Salamanca, Spain

Correspondence
César Roncero
crm@usal.es

In *Saccharomyces cerevisiae* cytokinesis is efficiently achieved when a concerted series of events take place at the neck region, leading to septum formation. Here it is shown that Bni4p plays a crucial role in this process. Δ*bni4* mutants contain normal amounts of chitin and show normal chitin synthase III (CSIII) activity, but are partially resistant to Calcofluor White (CFW), probably due to the striking pattern of chitin distribution. CFW vital staining shows that chitin is synthesized in daughter cells and that it is also asymmetrically deposited at the mother-side of the neck in large-budded cells. This specific pattern coincides with that of Chs4p and Chs3p proteins. Alternatively, staining of unbudded cultures confirmed that Bni4p directs early chitin ring assembly, but is no longer required for the chitin deposition that occurs late in the cell cycle at cytokinesis. Consequently, this work provides a strategy to genetically discriminate between the absence of chitin synthesis (Δ*chs3* mutant) and failure in chitin ring assembly (Δ*bni4* mutants). The characterization of double mutants affected in chitin synthesis and primary septum (PS) assembly (Δ*myo1* and Δ*chs2*) provides evidence for the cooperation of Bni4p in PS formation besides its role in chitin ring assembly. In addition, it is shown that the chitin ring, but not the late deposition of chitin, cooperates in the correct assembly of the actomyosin ring and the PS when the biological function of the septins is compromised. We conclude that Bni4p is not only required for the assembly of the chitin ring, but is also involved in septum architecture and the maintenance of neck integrity.

Received 21 May 2004
Revised 23 July 2004
Accepted 2 August 2004

INTRODUCTION

The fungal cell wall is a very important structure for cell survival because it confers on cells a rigid support that guarantees their shape while at the same time protecting them from aggressive environments. There must be specific mechanisms to promote cell wall synthesis at the growing part of the cell to ensure proper growth. Cell wall structure and composition are fairly uniform and hence a continuous supply of cell wall materials to growth sites might be sufficient to sustain the cell wall expansion required for cell growth (Cid *et al.*, 1995; Orlean, 1997). Such a process is guaranteed by the polarized trafficking of vesicles to the extension zone (Kaiser *et al.*, 1997). However, the uniformity of the *Saccharomyces cerevisiae* cell wall structure is lost at the cell division site (Cid *et al.*, 1995) where cells display the septum, a specialized structure of the cell wall that physically separates mother and daughter cells, allowing their separation without lysis (Cabib *et al.*, 1996).

Abbreviations: CFW, Calcofluor White; CSI, CSII, CSIII, chitin synthase I, II, III; GFP, green fluorescent protein; PS, primary septum; SS, secondary septum; TEM, transmission electron microscopy.

Cytokinesis in *S. cerevisiae* is properly achieved when three independent but concerted processes occur at the neck region, leading to septum formation (Cabib *et al.*, 1996; Bi, 2001). First, and very early in the cycle, a chitin ring is formed at the base of the emerging bud (Cabib *et al.*, 2001). Second, the contractile actomyosin ring guides centripetal invagination of the plasma membrane (Lippincott & Li, 1998) and, concomitantly, chitin synthase II (CSII) activity (Roh *et al.*, 2002) synthesizes the chitin disc known as the primary septum (PS) (Molano *et al.*, 1980). Finally, cell wall material is added from the mother and daughter cells and laid out over the PS, thus creating the secondary septum (SS), whose composition is not precisely known. Once the septum has been formed, cell separation is promoted by the action of hydrolytic enzymes from the daughter side of the cell (Baladron *et al.*, 2002; Colman-Lerner *et al.*, 2001), producing an asymmetric distribution of cell wall material that leaves most, if not all, chitin in the mother cell (Cabib *et al.*, 1996). To a certain extent, the structure of the bud scars reflects the story of the events leading to septum formation. The efficient completion of all these processes requires the involvement of the septin filament ring (for a review, see Longtine & Bi, 2003).

The chitin ring surrounds the three-layered structure formed by the PS and SS, conferring strength to the neck region. Recently, it has been shown that the chitin ring cooperates with the septin ring in maintaining neck integrity (Schmidt *et al.*, 2003). This ring is assumed to contain most of the cellular chitin, which constitutes the base of bud scars (Molano *et al.*, 1980). This chitin ring is synthesized by the action of chitin synthase III (CSIII) activity, which is subjected to complex regulation (Roncero, 2002). The catalytic subunit of CSIII is Chs3p, a protein whose levels do not change significantly during the cell cycle and whose intracellular trafficking is essential in the control of the activity. At different stages, anterograde transport of Chs3p depends on the Chs7p, Chs6p and Chs5p proteins, although endocytic recycling also appears to participate in CSIII regulation (for a review, see Roncero, 2002). Other key elements in CSIII regulation are Chs4p (Trilla *et al.*, 1997) and Shc1p (Sanz *et al.*, 2002), although the function of the latter is restricted to the sporulation process. The involvement of Chs4p in Chs3p trafficking is not well established. In contrast, it has been well documented that Chs4p acts as an activator of CSIII through an unknown mechanism (Choi *et al.*, 1994; Trilla *et al.*, 1997; Ono *et al.*, 2000). In addition, Chs4p plays an essential role in the correct positioning of CSIII at the neck site (DeMarini *et al.*, 1997). Chs4p interacts physically with Chs3p (DeMarini *et al.*, 1997; Ono *et al.*, 2000) and at the same time with Bni4p, a protein whose function is unknown but which appears to form part of the septum synthesis machinery (DeMarini *et al.*, 1997; Kozubowski *et al.*, 2003). The physical interaction between Chs4p and Chs3p would explain why these two proteins also depend on each other for correct localization.

PS formation requires CSII activity, whose catalytic subunit is encoded by *CHS2*, and Myo1p, the only type II myosin in *S. cerevisiae*, which is required for the function of the contractile ring. Both processes have been shown to be interdependent (Schmidt *et al.*, 2002). In the absence of the actomyosin ring (Δ*myo1* null mutants), cytokinesis is still accomplished, albeit less efficiently (Bi, 2001; Tolliday *et al.*, 2003). In Δ*chs2* mutants, the actin and Myo1p rings are formed but are unable to contract (Bi, 2001). In both cases cytokinesis is achieved through the formation of very thick, aberrant septa (Shaw *et al.*, 1991; Schmidt *et al.*, 2002; Tolliday *et al.*, 2003). These remedial septa require a functional CSIII activity, but not the chitin ring (Cabib & Schmidt, 2003).

Septins are involved in diverse processes, mainly acting as scaffolds for multiple proteins (Longtine & Bi, 2003). Very recently, it has been shown that septins participate in the recruitment to the septum of the actomyosin contractile machinery as well as of CSII activity, both directly involved in PS synthesis (Lippincott & Li, 1998; Bi, 2001; Schmidt *et al.*, 2002). In addition, the localization of Chs3p and Chs4p at the septum also depends on septins (DeMarini *et al.*, 1997). However, this interaction is not direct, but occurs through Bni4p, which in turn also interacts physically with the septin ring (DeMarini *et al.*, 1997). Preliminary evidence has suggested that Bni4p is required for correct chitin synthesis (DeMarini *et al.*, 1997; Kozubowski *et al.*, 2003).

Additional evidence concerning the involvement of Bni4p in chitin synthesis arises from a global study of synthetic interactions that has been published recently (Tong *et al.*, 2004). This work clearly shows that Bni4p and Chs3p participate in the same cellular process, cell wall synthesis, but also that both proteins must exert additional and independent functions.

Our work in the search for Calcofluor White (CFW)-resistant mutants (for a review, see Roncero, 2002) has led to the identification of a CFW-resistant *bni4* mutant, a result typically related to defects in chitin synthesis. Thus, in this report we reappraise the role of Bni4p by analysing the role of this protein not only in chitin synthesis but also in the construction of the yeast division septum.

METHODS

Strains, growth conditions and genetic methods. The yeast strains used in this work are listed in Table 1. *Saccharomyces cerevisiae* cells were grown in either YEPD (2 % glucose, 2 % peptone, 1 % Bacto yeast extract) or SC medium (2 % glucose, 0·7 % Difco yeast nitrogen base without amino acids and BIO 101 Complete Supplement Mixture (CSM) minus the appropriate amino acid). Agar (2 %) was added for solid media. *Escherichia coli* DH5α was used for routine propagation of plasmids and strain CJ236 (Bio-Rad) for site-directed mutagenesis. Luria–Bertani (LB) medium supplemented with 100 μg ampicillin ml^{-1} and 50 μg kanamycin ml^{-1} when appropriate was used to grow bacteria. Standard methods were used for DNA manipulations (Sambrook *et al.*, 1989) and yeast genetics (Rose *et al.*, 1990).

Sporulation was induced as described previously (Sanz *et al.*, 2002). In the case of diploids containing plasmids, pre-sporulation was carried out in media selective for leucine. Tetrad dissection was carried out in YEPD or in synthetic complete (SC) medium minus leucine when required. For plasmid-shuffling experiments, cells were grown in YEPD for approximately 30 generations by successive dilutions. After this, cell concentrations were determined with a haemocytometer. Appropriate dilutions of each culture were plated onto YEPD medium. The presence of the plasmid was monitored by growing isolated colonies in SC medium with or without leucine.

CFW resistance was assayed in SC solid media, supplemented with different CFW (Blankophor BBH; Bayer) concentrations (125–1000 μg ml^{-1}) as described previously (Sanz *et al.*, 2002).

Yeast strains construction. The null mutants generated in this work were obtained by the gene replacement technique as described by Rothstein (1983).

For the disruption of *BNI4*, two DNA fragments flanking the *BNI4* ORF were amplified by PCR from chromosomal DNA. The oligonucleotides used to amplify the 450 bp BNI4-N fragment were as follows: BNI4-N1 (***Xho*I**) 5′-A**CTCGAG**CAACCGTACCATTAAG-TG-3′ and BNI4-N2 (***Hin*dIII**) 5′-A**AAGCTT**GAAATACTATCCG-AC-3′. To amplify the 350 bp BNI4-C fragment, the oligonucleotides

Table 1. *S. cerevisiae* strains used in this study

Strain	Relevant genotype	Source
W303a	*MAT***a** *can1-100 ade2-1 his3-11,15 leu2-3,12 trp1-1 ura3-1*	Lab collection
W303α	*MATα can1-100 ade2-1 his3-11,15 leu2-3,12 trp1-1 ura3-1*	Lab collection
LJY35	W303a E5	Garcia-Rodriguez *et al.* (2000a)
CRM233	W303 *MATα chs4*::*HIS3*	Lab collection
CRM101	W303 *MAT***a** *chs3*::*URA3*	Lab collection
CRM103	W303 *MATα chs3*::*URA3*	Lab collection
CRM434	W303 *MAT***a** *bni4*::*URA3*	This study
CRM483	W303 *MATα bni4*::*URA3*	This study
CRM499	W303 *MATα chs4*::*HIS3 bni4*::*URA3*	This study
CRM278	W303 *MAT***a** *chs4*::*HIS3 chs3*::*LEU2*	Lab collection
Y1306	*MAT***a** *ura3 lys2 ade2 trp1 his3 CHS3*::*3xHA*	Santos & Snyder (1997)
CRM403	Y1306*MAT***a** *bni4*::*URA3*	This study
CRM787	W303 *MAT***a** *chs2*::*LEU2*	This study
CRM836	W303 *MAT***a** *chs2*::*LEU2 bni4*::*URA3*	This study
CRM834	W303 *chs2*::*LEU2 chs3*::*URA3*	This study
CRM 716	W303 *MATα myo1*::*HIS5*	This study
CRM830	W303 *myo1*::*HIS5 bni4*::*URA3*	This study
CRM828	W303 *myo1*::*HIS5 chs3*::*URA3*	This study
Y1783	*MAT***a** *ura3-52 leu2-3,112 trp1-1 his4 canR*	Cid *et al.* (1998)
VCY1	Y1783 *MATα cdc10-11*	Cid *et al.* (1998)
CRM820	Y1783 *MATα cdc10-11 bni4*::*URA3*	This study
CRM824	Y1783 *MATα cdc10-11 chs3*::*LEU2*	This study

used were: BNI4-C1 (***Hin*dIII**) 5′-A**AAGCTT**GGCTCAAATGATCA-AATTGG-3′ and BNI4-C2 (***Sal*I**) 5′-A**GTCGAC**AGGTATTCAATG-CTCTGG-3′. Both PCR products were cloned separately into pGEM-T vectors (Promega). In a second step, the BNI4-C fragment was cut with *Hin*dIII/*Sal*I and ligated into pGEM-BNI4-N previously digested with the same enzymes, obtaining pGEM-BNI4-N-C. Finally, a 1·2 kb *Hin*dIII–*Hin*dIII fragment containing the *URA3* marker was inserted into the *Hin*dIII site remaining between the BNI4-N and -C fragments, thus creating pGEM-*bni4*::*URA3*. Digestion of this plasmid with *Xho*I/*Sal*I released the 2·0 kb fragment containing the *bni4*::*URA3* deletion cassette, which was transformed into different yeast strains by the lithium acetate method. *URA3* prototrophs were selected and correct gene replacement was confirmed by PCR analysis.

Disruption of *MYO1* and *CHS2* in the W303 strain was performed using the same strategy. The *myo1*::*HIS5* deletion cassette was kindly provided by Dr Rodríguez-Medina (Universidad de Puerto Rico). The *chs2*::*LEU2* cassette was constructed by inserting the *LEU2* marker into a *Sal*I restriction site created between two fragments of 800 and 400 bp, corresponding to flanking zones, upstream and downstream, respectively, from the *CHS2* ORF inserted in a pKS vector that was kindly provided by Dr Valdivieso (Universidad de Salamanca, Spain). Subsequent digestion with *Bst*UI released the 3·0 kb fragment containing the *chs2*::*LEU2* cassette.

Strains Δ*myo1* Δ*bni4*, Δ*myo1* Δ*chs3* and Δ*chs2* Δ*chs3* were obtained by crossing isogenic W303 haploid strains containing the single deletions. Diploids were sporulated, tetrads dissected and spores were checked to select the double mutants, which were confirmed by PCR. To create the Δ*chs2* Δ*bni4* double mutant, strain CRM787 (*chs2*::*LEU2*) was transformed with the linear DNA fragment containing the *bni4*::*URA3* cassette. Strain *cdc10-11* (Cid *et al.*, 1998) was transformed with the linear DNA fragment containing the *bni4*::*URA3* cassette, yielding CRM820 (*cdc10-11* Δ*bni4*), and with the *chs3*::*LEU2* cassette, previously created in our laboratory, thus obtaining CRM824 (*cdc10-11* Δ*chs3*). Homologous recombination was always confirmed by PCR.

Plasmid construction. To construct plasmid pRS315::*CHS4*-GFP (green fluorescent protein), we used site-directed mutagenesis to introduce an in-frame *Nde*I site just after the ATG start codon of *CHS4* (oligonucleotide 5′-GGTGAACTTGC**CATATG**TTATCC-3′). Then, an *Nde*I–*Nde*I DNA fragment of 729 bp containing the E-GFP (Fernandez-Abalos *et al.*, 1998) coding sequence was cloned into this newly created site. Construction was confirmed by direct sequencing. The *CHS4*-GFP chimera was also cloned into the pRS314 vector. The Chs4p-GFP protein was confirmed to be fully functional by testing the complementation of the phenotypes associated with the Δ*chs4* deletion strain.

Plasmid pRS314::*MYO1*-GFP was constructed by digesting plasmid pRS315::*MYO1*-GFP (pLP8) (Lippincott & Li, 1998) with *Sal*I/*Not*I. The 6·7 kb fragment containing *MYO1*-GFP was treated with Klenow to create blunt-ends and ligated into the *Sma*I site of pRS314.

Chitin and CSIII determinations. Chitin was measured enzymically as described previously (Sanz *et al.*, 2002) using chitinase from *Serratia marcescens* (Sigma) and colorimetric determination of the total *N*-acetylglucosamine released.

CSIII activity determination was performed as described by Choi & Cabib (1994). The addition of Ni^{2+} and Co^{2+} cations to the reaction mixtures allowed specific measurement of CSIII activity in the presence of CSI and CSII activities. Different trypsin concentrations were assayed to determine the best proteolysis activation.

In both cases, the quantitative values are represented as the means of at least three independent experiments.

Preparation of samples for microscopy and image processing. For vital chitin staining with CFW, early-exponential-phase cells in YEPD liquid medium were supplemented with CFW (50 μg ml^{-1} final concn). After 2–3 h growth, samples were collected and immediately visualized using the appropriate UV filter (340–380 nm excitation and 425 nm emission wavelengths). Alternatively, early-exponential-phase cells were fixed and stained with CFW as described by DeMarini *et al.* (1997).

Isolation of unbudded (virgin) cells was achieved by centrifugation in a sucrose gradient as described by Schmidt *et al.* (2003). Cells were then incubated in YEPD medium in the presence of 50 μg CFW ml^{-1} at 28 °C. Every 20 min samples were removed, observed and counted to determine the synthesis of chitin rings.

To estimate cell viability in growing cultures, cells were collected, resuspended in 0·3 % methylene blue and immediately observed under bright-field microscopy. Cells stained blue were recorded as lysed cells.

Localization of Chs4p-GFP was observed directly in exponentially growing cells containing plasmid pRS315::*CHS4-GFP* using a specific GFP filter (GFP blue, 470–440 nm excitation and 525–550 nm emission wavelengths). Indirect immunofluorescence was used to localize Chs3p-3XHA and Cdc11p intracellularly as described by Garcia-Rodriguez *et al.* (2000b). Mouse HA.11 anti-HA (BabCo), diluted 1 : 75, and Cdc11(y-415) anti-Cdc11 (Santa Cruz Biotechnology), diluted 1 : 150, were used as primary antibodies. Alexa Fluor 594 anti-mouse and Alexa Fluor 488 anti-rabbit, diluted 1 : 400, were used as secondary antibodies, respectively.

All microscopic techniques were performed with a Leica RX150 photomicroscope, using an epifluorescence system with a 100 W Hg lamp. Phase-contrast, bright-field and CFW fluorescence images were obtained with a Leica DC 100 digital camera. For GFP and immunofluorescence, a Sensys (Photometrics) digital camera and Leica QFISH V2.3a software were used. Digital photographs were processed using the Adobe Photoshop 5.0 software package.

Electron microscopy. Transmission electron microscopy (TEM) was performed essentially as described by Wang *et al.* (2002). Briefly, *S. cerevisiae* cultures were grown to an OD_{600} of 0·5–1·0. Then, 12·5 OD_{600} units of cells were collected by centrifugation, washed and fixed in 2 % potassium permanganate for 1 h at room temperature. Excess potassium permanganate was removed by exhaustive washing and stained cells were finally dehydrated by incubation in increasing concentrations of ethanol. Samples were processed in the embedding medium (Spurr Resin Embedding Kit; TAAB) by successive 2 h incubations in 1 : 1 and 1 : 3 ethanol/embedding medium mixtures and, finally, in fresh embedding medium. Cells were concentrated in 500 μl resin and were allowed to polymerize overnight at 60 °C. Ultrathin sections were obtained using an LKB Ultratome III microtome and samples were visualized under a Zeiss EM900 transmission electron microscope.

RESULTS

Δ*bni4* mutants contain normal amounts of chitin and CSIII activity, but chitin deposition is altered

Previous work in our laboratory led to the isolation of several mutants resistant to 0·5 mg CFW ml^{-1}. Some of them showed apparently normal amounts of chitin and their characterization indicated that most contained mutations in the high-osmolarity glycerol response (HOG) signal transduction pathway (Garcia-Rodriguez *et al.*, 2000a). However, mutant E5 showed specific characteristics since it was resistant to high salt concentrations and was not affected in the HOG pathway. To understand the nature of this mutation, the E5 mutant was transformed with a centromeric genomic bank (Rose *et al.*, 1987) and tested for complementation of the resistance phenotype. CFW resistance was complemented by a plasmid containing an insert of approximately 10 kb from chromosome XIV, encoding seven proteins. Subcloning experiments showed that the complementing ORF was YNL233W (*BNI4*) (results not shown), a gene previously described as being involved in Chs4p and Chs3p intracellular localization (DeMarini *et al.*, 1997). These results prompted us to reassess the role of Bni4p in chitin synthesis.

The Δ*bni4* null mutant (see Methods for details of construction) was resistant to low CFW concentrations. However, growth at high CFW concentrations (1 mg ml^{-1}) was significantly diminished with respect to that of the Δ*chs4* mutant or other Δ*chs* mutants deficient in chitin synthesis (not shown). Accordingly, Δ*bni4* cells appeared to contain chitin, as determined by CFW staining (Fig. 1a, b). CFW staining of fixed cells revealed a rather uniform chitin distribution across the mother cell surface (Fig. 1b), in agreement with previous reports (DeMarini *et al.*, 1997). However, vital staining with CFW (Fig. 1a) (see Methods for details) allowed clearer discrimination between wild-type (wt) and Δ*bni4* cells. In wt cells most chitin was accumulated at the septum between the mother and daughter cells, while in Δ*bni4* cells a significant number of buds showed a defined staining pattern, indicating that chitin synthesis was occurring actively in the daughter cells. In addition, chitin deposition at the neck appeared altered in the Δ*bni4* mutant.

To characterize chitin deposition more precisely, CFW staining was performed in cultures enriched with unbudded cells (see Methods). In wt cells, the accumulation of chitin at the neck region occurred very early after the budding process had been initiated and persisted during the cell cycle (Fig. 1c, upper panels). After 60 min incubation, virtually the whole cell population showed chitin deposition at the mother–daughter junction (Fig. 1d). In Δ*bni4* cells, chitin synthesis was also initiated early during the cell cycle, but its deposition at the neck was altered significantly. In this mutant, early chitin deposition occurred mostly at the bud instead of at the neck and only large-budded cells showed chitin staining at the neck (Fig. 1c, lower panels). Chitin deposition at the neck was delayed, with a maximum after 120 min, and it was only detected in a small proportion of the population (30 %) (Fig. 1d), corresponding to a significant part (60 %) of the large-budded cells. Apparently, this type of deposition is restricted to a late and short part of the cell cycle, probably associated with SS assembly at the time of cytokinesis.

Further observation of the vitally stained cells suggested that chitin deposition at the neck in the Δ*bni4* mutant

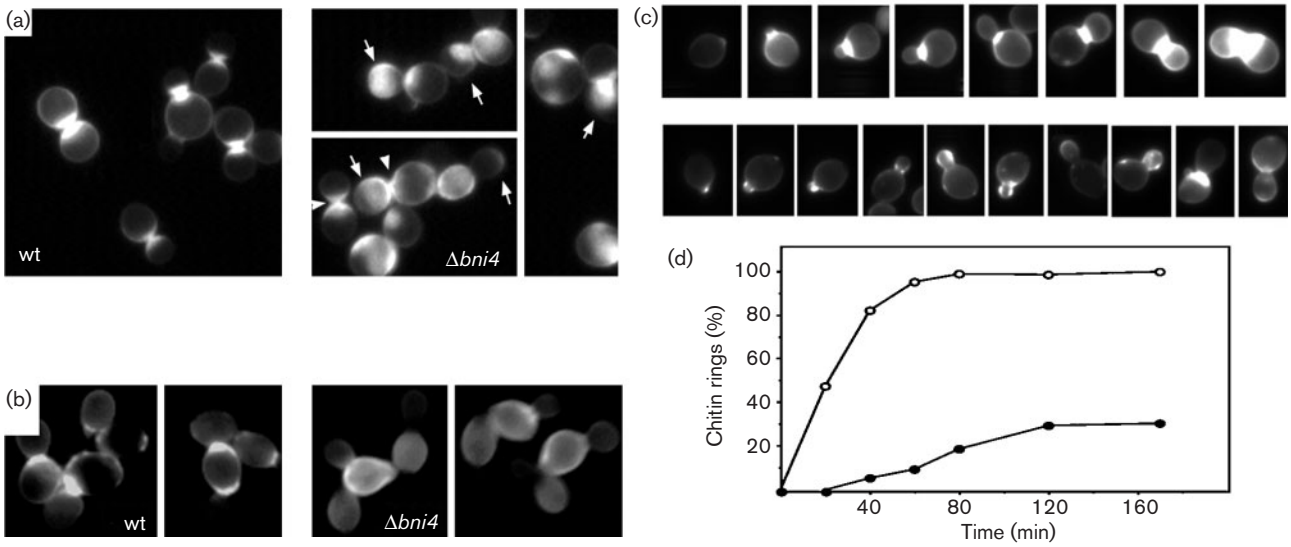

Fig. 1. Distribution of chitin after CFW staining. (a) Vital staining of wt and mutant cells after 3 h growth. Arrows mark stained buds. Arrowheads indicate chitin deposition at the neck. (b) CFW staining of fixed cells. Note the uniform stain of the mother cells in the Δ*bni4* mutant and the absence of bud staining. (c) CFW vital staining of unbudded cells showing the accumulation of chitin along cell cycle progression. Upper panels show wt cells and lower panels Δ*bni4* cells. Cell cycle progression is shown from left to right. (d) Percentage of the total population that shows chitin deposition at the neck during cell cycle progression in the synchronized cultures used for the images in (c). Open circles, wt; filled circles, Δ*bni4*.

occurred mostly at the mother-side of the neck (Fig. 2a), contrary to what was observed in the wt cells, where chitin appeared to be deposited symmetrically at both sides of the neck. TEM of these cells confirmed these results since CFW treatment of wt cells produced an increased deposition of cell wall material symmetrically to the neck, in agreement with a previous report (Roncero & Duran, 1985) (Fig. 2b). In Δ*bni4* cells, cell wall deposition after CFW was only increased at the mother-side (Fig. 2b).

Taken together, all these observations indicated that septum structure must be different between wt and Δ*bni4* cells, as confirmed later.

Despite the described defects in chitin deposition, chitin synthesis was not quantitatively reduced in the Δ*bni4* mutant; instead, we observed a modest but significant increase in chitin levels compared with the control (Table 2). CSIII activity was fairly similar to that of the control strain and it did not display the zymogenic character observed in the Δ*chs4* mutant (Table 2 and Trilla *et al.*, 1997). No additive effects on chitin synthesis or CSIII activity were observed in the double Δ*chs4* Δ*bni4* mutant (Table 2). These results indicate that the presence of Bni4p is not required for the synthesis of fully functional CSIII activity as other *CHS* products are.

Localization of Chs4p and Chs3p is altered in Δ*bni4* mutants

CSIII activity depends on the function of Chs4p and Chs3p, but previous studies have indicated that Chs4p interacts

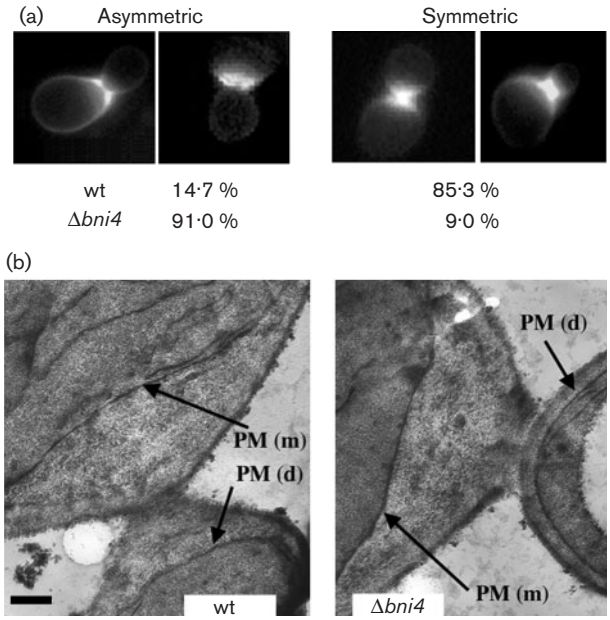

Fig. 2. Chitin distribution at the neck determined after CFW vital staining (a) or TEM (b). (a) Chitin deposition occurs asymmetrically at the mother-side of the neck in most Δ*bni4* cells ($n>100$), but symmetrically in wt cells ($n>100$). (b) TEM images of wt and Δ*bni4* cells after CFW treatment. Note the symmetric accumulation of cell wall material in wt cells while in the mutant the accumulation occurs only at the mother-side of the neck. The plasma membranes (PM) of the mother (m) and daughter (d) cells are indicated for reference. Bars, 0·25 μm.

Table 2. Chitin synthesis in the Δ*bni4* mutant

Strain	Chitin content (%)*		
Wild-type	422·2±19·4 (100·0)		
Δ*chs4*	56·4±13·0 (13·3)		
Δ*bni4*	515·2±86·3 (122·0)		
Δ*chs4* Δ*bni4*	70·6±3·2 (16·7)		
	Chitin synthase III activity†		
	Basal	Total	Activation factor
Wild-type	9·2±2·1	30·6±10·0	×3·3
Δ*chs4*	4·6±0·9	24·6±13·9	×5·3
Δ*bni4*	9·3±2·3	29·9±11·2	×3·2
Δ*chs4* Δ*bni4*	6·9±1·1	34·7±17·7	×5·0

*Chitin content was determined as described in Methods. Values are expressed as nmol *N*-acetylglucosamine per 100 mg wet wt cells and as a percentage relative to the control strain.
†CSIII activity was determined before (basal) or after trypsin treatment as described by Choi & Cabib (1994). Values are expressed as mU h^{-1} (mg protein)$^{-1}$. Activation factor represents the increase in activity after trypsin treatment.

with Bni4p and that this interaction is responsible for the chitin accumulation at the neck (DeMarini *et al.*, 1997; Kozubowski *et al.*, 2003).

Since our results partially differed from previous reports, we investigated Chs4p localization under our experimental conditions using a fully functional *CHS4*-GFP chimera that was introduced into different strains in a centromeric plasmid (see Methods). In wt cells, Chs4p accumulated at the presumptive budding site and at the neck in small-budded cells. Further progression of the cycle expanded the localization of Chs4p and, occasionally, two rings were visible at both sides of the neck (Fig. 3a). Conspicuously, in medium-budded cells the population of cells showing Chs4p-GFP localization was reduced compared to other cell cycle stages (data not shown). A similar pattern of localization has been observed for Chs3p (Santos & Snyder, 1997; and data not shown).

Δ*bni4* cells also showed discrete Chs4p localization (Fig. 3a). However, Chs4p accumulation at the base of small-budded cells was essentially absent; instead, a significant number of buds showed Chs4p localization along their surfaces (see table insert in Fig. 3a). Compared to wt, the number of large-budded cells showing Chs4p localization at the neck did not differ significantly, and neither did the total amount of cells showing Chs4p localization. Apparently, Bni4p is required for correct Chs4p localization during the initial part of the cell cycle, but is not required for the accumulation of Chs4p at the neck during cytokinesis. Furthermore, the localization of Chs4p during bud emergence, but not at cytokinesis, depends partially on Chs3p (Fig. 3a, inserted table), a clear indication that the

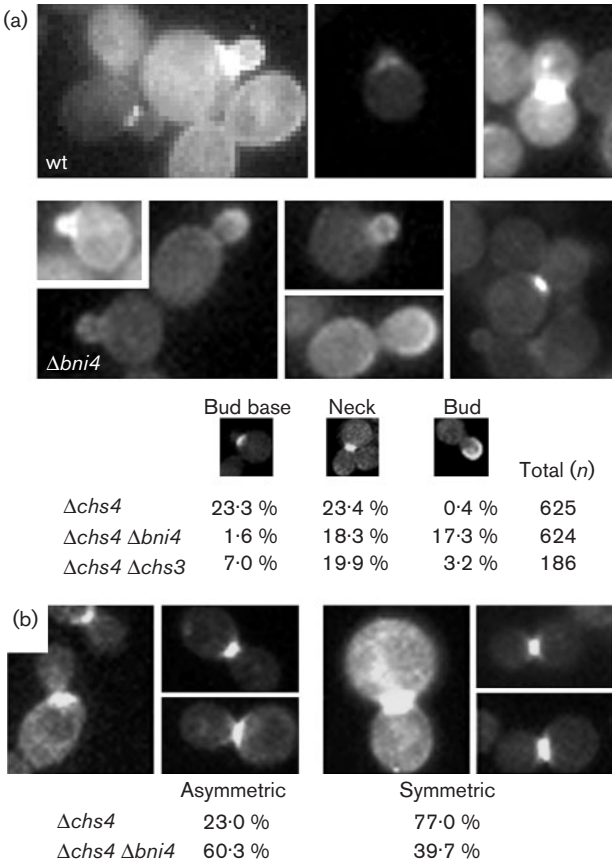

Fig. 3. Chs4p-GFP distribution in different mutants. (a) Selected images showing Chs4p-GFP localization at different cell cycle stages and quantitative analysis of Chs4p distribution. Data are expressed as percentages of cells showing the specific distribution recorded: bud base, neck and bud surface. Note the characteristic bud distribution of Chs4p in the Δ*bni4* mutant. (b) Quantitative analysis of Chs4p localization at the neck in the population of large-budded cells. Symmetric and asymmetric distributions were recorded ($n > 200$).

Chs3p/Chs4p interaction is also involved in the process. In addition, in large-budded cells Chs4p localization at the neck in Δ*bni4* cells occurred mostly at the mother-side and not symmetrically, as it occurs in the wt (Fig. 3b).

From the above results it may be concluded that there is a perfect relationship between Chs4p localization and chitin deposition, strongly supporting the notion that the delocalized deposition of chitin observed in Δ*bni4* cells must be mainly due to the altered localization of Chs4p.

The absence of Bni4p alters SS structure

Septum formation at the bud neck is a crucial step in cell division in yeast. This structure is reinforced by the early synthesis of the chitin ring that constitutes the base of the bud scars. Observation of recent bud scars under TEM showed the chitin ring as a translucent zone at both sides

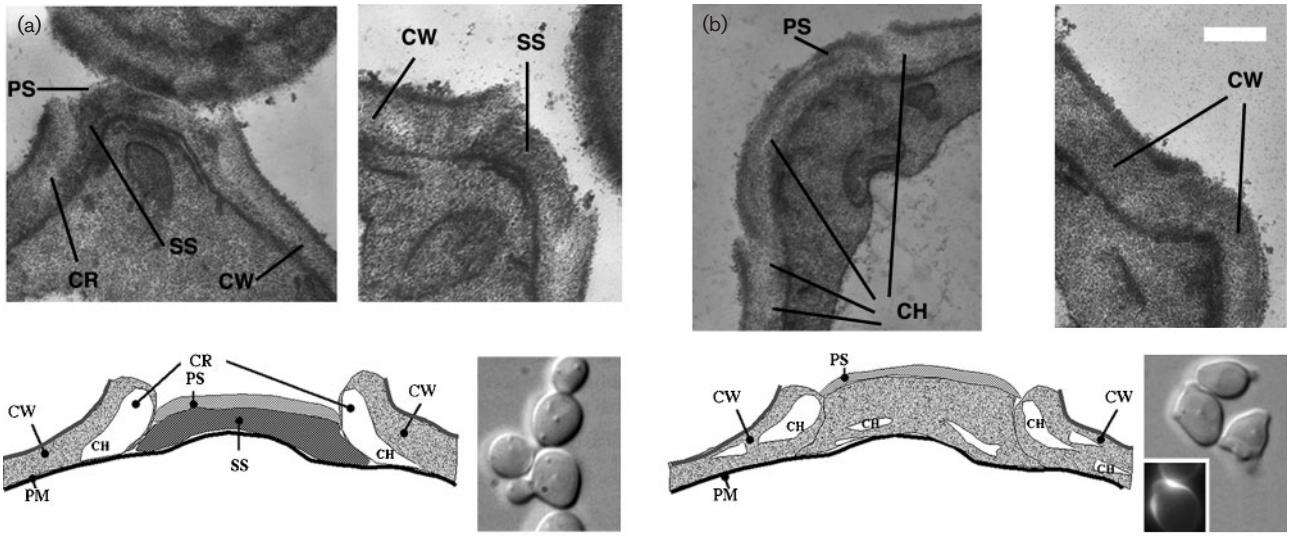

Fig. 4. TEM of septum and bud scars from the wt (W303) (a) and the Δ*bni4* mutant (CRM483) (b). The results are represented in the lower part as a schematic drawing showing the different structures observed in the TEM images. Note the absence of the darker zone (SS) under the PS in the mutant cells. The smaller pictures show DIC and fluorescent images obtained in a light microscope. The fluorescence shows chitin distribution after CFW vital staining. Bars, 0·25 μm. Abbreviations: CW, cell wall; PM, plasma membrane; CH, chitin; CR, chitin ring.

of the scar (Fig. 4a; see also Cid *et al.*, 1995). The chitin ring delimited a darker zone that was clearly different from the surrounding cell wall. This cell wall portion could be interpreted as the SS, whose exact composition remains uncertain. The most external part of the bud scar was the PS, made of chitin synthesized by CSII (see Fig. 4a for details).

Since the deposition of chitin in the Δ*bni4* mutant seemed peculiar, we also determined the structure of the septum in this mutant. Translucent zones were also observed (Fig. 4b), but they were diffuse and spread out, indicating a wider distribution of chitin. In addition, the darker zone below the PS was not observed since this zone appeared as a direct extension of the lateral cell walls. These alterations produced more prominent bud scars, which were clearly visible under the light microscope (compare small photographs in Fig. 4) or after CFW staining. No marked differences were observed at the level of the PS.

In conclusion, Bni4p is required for the correct synthesis of the chitin ring, but it is also required for the deposition and/or assembly of the SS material. Whether this phenotype is directly or indirectly related to the absence of Bni4p remains to be elucidated (see Discussion for further comments).

Relationship between Bni4p and PS synthesis

All the data gained so far for Δ*bni4* cells pointed to a direct involvement of Bni4p in the construction of the chitin ring, but not in the chitin synthesis process, which is not affected. Thus, this mutant provided an excellent tool to genetically discriminate between both situations: the absence of chitin synthesis (Δ*chs3*) and the absence of chitin ring assembly (Δ*bni4*). Therefore, we investigated the relationship between the assembly of the chitin ring and the formation of the PS by constructing a set of Δ*bni4* and Δ*chs3* double mutants combined with isogenic PS-deficient strains (Δ*myo1* and Δ*chs2*). After tetrad dissection ($n=44$) the number of Δ*myo1* Δ*bni4* colonies obtained was only 20 % of that expected. Rescue of double mutants increased to the expected levels when the diploid dissected contained the *MYO1* gene in a plasmid (data not shown). In addition, we were unable to cure (frequency $<0{\cdot}8$ %) the *MYO1*-containing plasmid in the double mutants obtained. The simultaneous loss of Bni4p and Myo1p apparently compromised cell growth. Surprisingly, double Δ*myo1* Δ*chs3* mutants were obtained with the same frequency as the single Δ*myo1*, suggesting no additional cell growth defects in this double mutant. The differences were confirmed by comparative growth analysis between the different mutants. Δ*myo1* Δ*bni4* cells grew poorly, clumpy and had aberrant morphologies, and they showed high levels of lysis after methylene-blue staining (Fig. 5a). In contrast, Δ*chs3* Δ*myo1* cells grew essentially as the single Δ*myo1* mutant and showed very reduced levels of lysis. The differences were independent of the growth medium (Fig. 5a).

Δ*chs2* Δ*bni4* and Δ*chs2* Δ*chs3* double mutants were, to our surprise, viable. However, they grew very slowly in both complex and defined media (not shown). The cells were heavily aggregated and showed a significant degree of lysis, a clear indication that growth was as compromised as in the double Δ*myo1* Δ*bni4* mutant (Fig. 5a). Nevertheless, the cell morphology of Δ*chs2* Δ*bni4* was relatively normal.

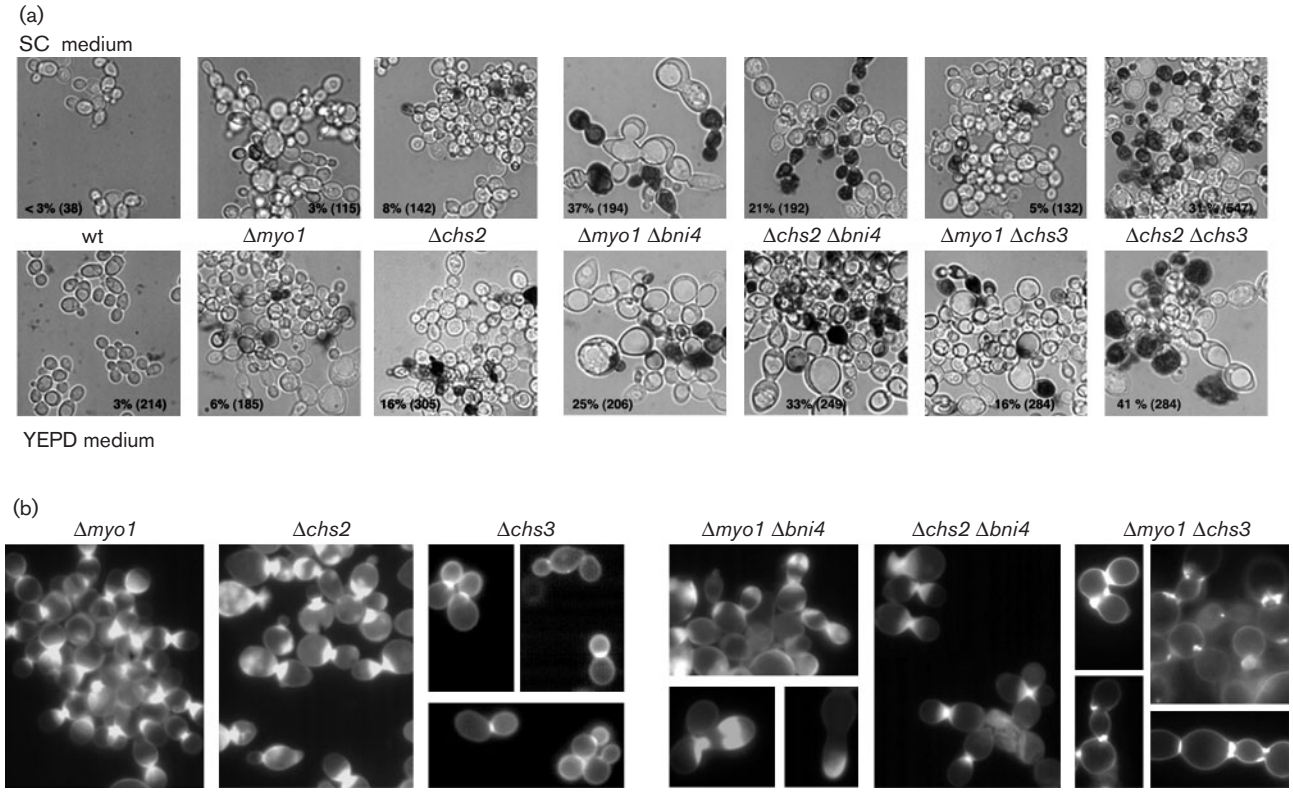

Fig. 5. Cellular morphology and chitin distribution in different strains. (a) General aspect of cultures of the indicated strain in SC or YEPD media after methylene-blue staining. Overlaid numbers indicate the percentage of cell lysis. The number of cells counted in each case is indicated in parentheses. (b) Vital CFW staining of the indicated strains. Note the difference in chitin deposition (see text). Images of all Δ*chs3* strains are overexposed to show details.

CFW staining shows that the Δ*myo1* and Δ*chs2* single mutants synthesized the thick and symmetric remedial septa characterized by the accumulation of chitin (Fig. 5b). As expected, the Δ*chs3* single mutant only formed the PS. The accumulation of chitin in the Δ*myo1* Δ*bni4* mutant indicated that the formation of the septum was the additive result of the single mutations: chitin deposition at the neck appeared abnormal and chitin synthesis also occurred at the growing bud. However, Δ*chs2* Δ*bni4* cells were very similar in appearance to the single Δ*chs2* mutant, with the synthesis of a symmetric remedial septum (Fig. 5b). Apparently, the absence of Myo1p and Chs2p produces different defects in septum assembly that are only apparent in the absence of Bni4p.

Δ*myo1* Δ*chs3* cells synthesized only the chitin corresponding to PS, but the absence of the contractile ring prevented the correct synthesis of the PS. However, the abnormal accumulation of chitin (Fig. 5b) produced by CSII provided a functional septum, which would explain the fairly normal growth of this double mutant. Comparison of growth, morphology and septum assembly between the Δ*myo1* Δ*bni4* and Δ*myo1* Δ*chs3* mutants suggests that Bni4p could play additional roles in septum formation other than directing the assembly of the chitin ring.

Bni4p is required for PS assembly when septin function is compromised

Using the same rationale as before, we wished to explore the possibility of a relationship between the synthesis of the chitin ring and the assembly of septins. To accomplish this, we constructed the double mutants *cdc10-11* Δ*bni4* and *cdc10-11* Δ*chs3* (see Methods for details). Growth of these double mutants at different temperatures was not significantly different from that observed for the *cdc10-11* single mutant (data not shown). However, the morphologies of both double mutants cells were significantly altered, even at 25 °C, a permissive temperature for the *cdc10-11* mutation (Fig. 6). Characterization of the septin ring assembly in this mutant by immunofluorescence with the anti-Cdc11p antibody or by fluorescence microscopy with the Cdc3p-GFP construction (Schmidt *et al.*, 2003) indicated that the original single mutant had a significant defect in septin assembly at 25 °C as determined by the reduced number of cells showing the septin ring as well as the reduced amount of septins assembled (data not shown). This result suggests that this mutation probably leads to a loss of function. No additional effects on septin assembly were observed in the corresponding double mutants as compared to the single *cdc10-11* mutant (data

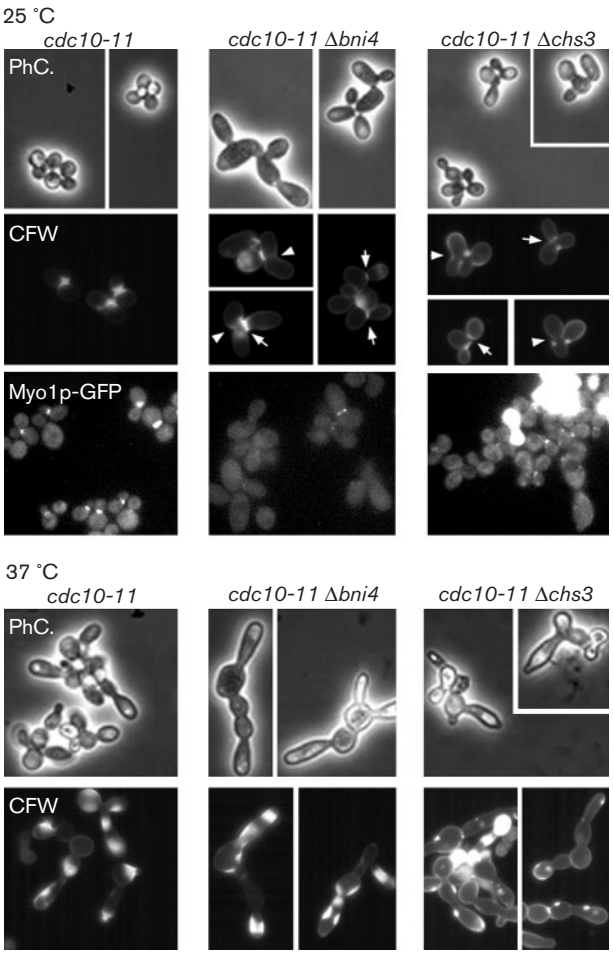

Fig. 6. Microscopic analysis of the indicated strains grown at the permissive (25 °C) and non-permissive (37 °C) temperatures. Cells were grown in YEPD medium and observed by phase-contrast (PhC.) or after CFW vital staining as indicated. When possible, chitin deposition at the PS is indicated as complete (arrows) or incomplete (arrowheads) septa. Images of all Δ*chs3* strains are overexposed to show details. Intracellular localization of Myo1p-GFP is also shown in cells growing at 25 °C. Note the reduced number of cells showing staining.

not shown). Incubation of all these mutants at the non-permissive temperature (32–37 °C) stopped growth and the mutants displayed the characteristic phenotypes associated with the complete loss of the septin ring.

The single *cdc10-11* mutant grew normally at 25 °C and the septum was formed normally as judged by CFW staining (Fig. 6). Accordingly, the assembly of the actomyosin ring, determined by use of the *MYO1*-GFP chimera, appeared normal (Fig. 6). However, on the basis of the lower fluorescence observed and the high number of cells without staining, in both the *cdc10-11* Δ*bni4* and *cdc10-11* Δ*chs3* double mutants, the assembly of the Myo1p ring was significantly reduced. Consequently, assembly of the PS was altered in the double mutants as judged by the high number of cells that lacked the chitin disc that separates mother and daughter cells after CFW staining. Nevertheless, the altered cellular morphology was always more apparent in the *cdc10-11* Δ*bni4* mutant than in the *cdc10-11* Δ*chs3* mutant. To confirm these findings, we measured the neck diameter in several mutants (Schmidt *et al.*, 2003). At 25 °C the neck diameter was similar in the wt, Δ*chs3*, *cdc10-11* and Δ*bni4* strains ($3{\cdot}34 \pm 0{\cdot}15$; $n > 50$ for each strain) and it did not change with an increase in temperature, except for the *cdc10-11* mutant at the non-permissive temperature (37 °C) ($3{\cdot}78 \pm 0{\cdot}64$, $n = 49$). At 25 °C the neck diameter of the double *cdc10-11* Δ*chs3* was similar to the control ($3{\cdot}14 \pm 0{\cdot}62$, $n = 46$), but the neck of the *cdc10-11* Δ*bni4* mutant was significantly enlarged ($4{\cdot}03 \pm 0{\cdot}96$, $n = 45$). Growth at the non-permissive temperature significantly increased the neck diameter in both double mutants (not shown).

These results indicate that both the chitin and septin rings cooperate together in the assembly of the actomyosin ring and hence in the formation of the PS. Additionally, Bni4p probably plays additional roles in the assembly of this structure apart from its involvement in chitin ring assembly.

DISCUSSION

Bni4p directs proper chitin ring assembly

Previous studies have reported indirect evidence implicating Bni4p in the regulation of chitin synthesis through its interaction with Chs4p and the septin ring (DeMarini *et al.*, 1997). However, more direct evidence can be gained from the results reported in this manuscript after characterization of the CFW-resistant mutant E5 (Garcia-Rodriguez *et al.*, 2000a) which proved to be affected in the *BNI4* gene. This mutation was probably not recovered in previous screenings since deletion of *BNI4* only produces resistance to moderate CFW concentrations, in contrast to other *chs* mutations. Accordingly, Δ*bni4* cells contain normal amounts of chitin and CSIII activity, and hence resistance is probably due to the delocalization of chitin (see below), which presumably alters the interaction of this polymer with CFW.

In previous studies, CFW staining of fixed cells indicated that chitin was distributed diffusely in Δ*bni4* cells (see Fig. 1b; DeMarini *et al.*, 1997; Kozubowski *et al.*, 2003). However, the vital CFW staining used in the present study shows that although chitin distribution is altered, it is not uniformly distributed in the mutant cells, but mislocalized (compare images in Fig. 1a and b), thus indicating that *S. cerevisiae* cells can partially direct chitin deposition in the absence of Bni4p. The differences observed between both CFW staining methods suggest that vital staining highlights the site of active chitin synthesis, allowing a better interpretation of what is happening in the cell. Alternatively, the use of synchronous cultures provides a more precise way of knowing how chitin deposition occurs during the cell cycle. In wt cells, the deposition of chitin at the neck

occurs very early on, and this chitin is assumed to constitute the chitin ring structure. Also, it has been proposed that additional accumulation of chitin at the neck takes place late in the cycle (Cabib & Schmidt, 2003), which would account for the accumulation of chitin in large-budded cells. However, neither CFW staining (Fig. 1) nor TEM (Fig. 2) allows easy discrimination between both rounds of synthesis.

The early accumulation of chitin in Δ*bni4* cells must be altered since no chitin ring was observed during the early stages of budding (Fig. 1c). Additionally, the bud surface showed chitin synthesis, which is seldom observed in the wt. An explanation for this could be that chitin synthesis occurs normally, but that the chitin ring is not properly assembled, indicating a direct role for Bni4p in chitin ring assembly. Nevertheless, chitin deposition at the neck was still observed in large-budded cells, suggesting that this deposition would be independent of Bni4p. Fluorescence and TEM clearly revealed that such deposition occurred specifically at the mother-side of the neck in Δ*bni4* cells. Moreover, Fig. 1(d) shows that this deposition is produced late during the cell cycle. These results indicate that this chitin accumulation is originated once the mother and daughter cells have become physically separated by the PS and is therefore probably related to construction of the SS.

In conclusion, the results discussed so far indicate that Bni4p has a direct role in the assembly of the chitin ring, but not in the late deposition of chitin that presumably corresponds to the formation of the SS. Thus, indirectly, through the Δ*bni4* mutant, we have obtained an easy way to experimentally separate the two rounds of chitin synthesis.

The localization of Chs4p in the different strains matches the sites of chitin deposition precisely, proving that proper Chs4p localization also depends on Bni4p. This dependence is only apparent during the initial stages of the cell cycle, since the localization of Chs4p during cytokinesis is not altered in Δ*bni4*, confirming an earlier report (Kozubowski *et al.*, 2003). Interestingly, it has been proposed, and later confirmed, that Chs4p disappears from the neck region during the medial part of the cell cycle (Kozubowski *et al.*, 2003). This result is in clear accordance with the pattern of chitin deposition observed by us, thus explaining the two temporally separated rounds of chitin deposition. In this scenario it is not surprising that chitin deposition only depends on Bni4p during part of the cell cycle.

Bni4p is not necessary for CSIII activity, but does participate in the anchorage of CSIII to the neck during bud emergence. In the absence of Bni4p, the Chs3p/Chs4p interaction occurs normally, but the active CSIII is moved towards the bud surface, probably through polarization mechanisms, until neck closure is achieved. Interestingly, our results also show that the Bni4p/Chs4p interaction partially depends on Chs3p, in agreement with an earlier report (DeMarini *et al.*, 1997). This suggests that the Chs3p/Chs4p interaction precedes its anchoring to the septin ring and would explain why Bni4p is not involved in CSIII regulation. Arrival of Chs4p at the membrane seems to be essentially independent of Chs3p, indicating that Chs4p has its own signals for membrane localization and that the interaction with Chs3p would occur very late during the intracellular protein sorting.

A recent report on synthetic lethality in *S. cerevisiae* (Tong *et al.*, 2004) has provided indirect confirmation of our results since the synthetic lethality observed for Δ*bni4* and Δ*chs3* mutants was significantly overlapped. Not surprisingly, the importance of chitin synthesis extends beyond the assembly of the chitin ring since the number of synthetic interactions of Δ*chs3* is much higher. In addition, Δ*bni4* shows exclusive lethal interactions, possibly pointing to additional functions of Bni4p (see below).

Bni4 is directly involved in septum architecture

TEM observations indicate that, in comparison with the wt, Δ*bni4* cells appear to lack the chitin ring, but the translucent zones observed along the neck (Fig. 4b) confirm that chitin deposition still occurs at the neck. However, the most significant difference observed was that Δ*bni4* cells conspicuously lacked the darker cell wall zone surrounded by the chitin ring that was easily recognized in the wt (see Fig. 4, but also Cid *et al.*, 1995). This zone corresponds to the SS, and so it seems to be clear that Δ*bni4* cells have an altered SS structure. Although this defect could be an indirect effect of the absence of the chitin ring, it is very likely that Bni4p also plays a role in SS formation by targeting other proteins. A feasible candidate could be Crh2p, presumably involved in the formation of transglycosidic linkages (see below) and whose precise localization to the neck at cytokinesis has been shown to depend on Bni4p (Rodriguez-Pena *et al.*, 2002).

If the only role of Bni4p were the assembly of the chitin ring, then Δ*bni4* should behave similarly or even better than Δ*chs3* mutations in combination with other mutations affecting septum assembly. However, the Δ*myo1* Δ*chs3* mutant behaved significantly better than the Δ*myo1* Δ*bni4* mutant. The former grew almost normally and with a very reduced level of lysis, suggesting that Δ*myo1* Δ*bni4* cells would contain additional defects that cannot be attributed to the role of Bni4p on chitin synthesis. The overall function of Bni4p is not completely understood, but it is required for the proper localization of Crh2p at the neck (Rodriguez-Pena *et al.*, 2002). This protein is probably responsible for part (Rodriguez-Pena *et al.*, 2000) of the glycosidic linkages between chitin and glucans (Kollar *et al.*, 1995). Therefore, the absence of such activity in Δ*bni4* mutants would be an attractive hypothesis to account for the different phenotypes observed. Since the discovery of the major *in vivo* CS activity, CSIII, it has been assumed that such linkages are related to this activity; however, if this were the case, the Δ*myo1* Δ*bni4* and Δ*myo1* Δ*chs3* mutants

should behave similarly, which is not the case. Therefore, our results point to another CS activity, CSII, as being responsible for the synthesis of the chitin serving as the substrate for the transglycosidic linkages that would form part of the PS. In this case, the Δ*myo1* Δ*chs3* double mutant would assemble primary septa incorrectly (see Fig. 5b), but the CSII activity, together with the correctly formed transglycosidic linkages, would allow the synthesis of a functional septum that would support the fairly normal growth of these cells. The participation of other transglycosidases in the construction of the septum remains to be tested.

In conclusion, these observations indicate that, in the absence of the actomyosin ring, CSIII activity is not the key element in constructing a remedial septum, but CSII, which along with Bni4p would cooperate in such a process, plays an essential role in achieving cytokinesis. In the course of our work, appearance of the Δ*chs2* Δ*chs3* double mutant, which lacks chitin and was originally described as lethal (Shaw *et al.*, 1991), was rather surprising. This mutant, as well as the Δ*chs2* Δ*bni4* double mutant, showed severe growth problems. In this situation, the presence of the actomyosin ring would serve to recruit alternative cell wall material at the neck for supporting deficient cell division. Despite the apparently normal localization of Myo1p-GFP in the Δ*bni4* mutant (data not shown), we cannot rule out a direct role of Bni4p in the function of the contractile actomyosin ring. Such a hypothesis would be in accordance with the synthetic lethality between *BNI4* and *CYK3* and *SEP7*, two genes that encode proteins involved in cytokinesis (Tong *et al.*, 2004).

Growth of the Δ*myo1* Δ*bni4* and Δ*chs2* Δ*bni4* double mutants was severely compromised, but chitin distribution in both mutants was significantly different. The Δ*myo1* Δ*bni4* phenotype resulted in the accumulation of Δ*myo1* and Δ*bni4* defects. Consequently, many cells failed to assemble the remedial septum required, thus producing very elongated cells (Fig. 5b). Surprisingly, the septa appeared enlarged, but rather normal in the Δ*bni4* Δ*chs2* double mutant and cell shape was apparently normal. In this mutant the presence of the actomyosin ring was apparently enough for recruiting the machinery that forms the remedial septa. Such recruitment must occur very early on during the cell cycle since virtually no chitin was observed in the bud despite the Δ*bni4* mutation. The differences observed between both double mutants are in contrast with the general belief that Δ*myo1* and Δ*chs2* mutations produce essentially the same phenotype (Schmidt *et al.*, 2002). Our results support the hypothesis that the functional contribution of Myo1p and Chs2p to the PS assembly would be different, as would be expected from two proteins with completely unrelated biochemical functions.

Bni4p participates in the maintenance of neck integrity

It has been reported that the chitin ring and septins cooperate in the maintenance of neck integrity (Schmidt *et al.*, 2003). During the course of this work we confirmed this by using a genetic strategy involving the characterization of different double mutants. The *cdc10-11* mutation, although described as temperature-sensitive (Cid *et al.*, 1998), proved to be a loss of function since septin assembly is compromised at the permissive temperature; therefore, the synthetic phenotypes observed when combined with Δ*bni4* or Δ*chs3* mutations were apparent even at 25 °C. In terms of growth and PS formation, both double mutants behaved similarly. The cells were elongated as compared to single mutants and they frequently failed to form the chitin disc that physically separates mother and daughter cells; i.e. the PS. This failure was probably due to the fact that the actomyosin ring was not properly assembled, as judged by Myo1p-GFP localization (Fig. 6). The fact that single mutants did not show these phenotypes strongly supports a model in which the septin and chitin rings would cooperate to ensure the neck integrity required for PS assembly. Apparently, the synthesis of bulk chitin is irrelevant in the process. The phenotypes of the double mutants cannot be attributed to additional defects of Bni4p or Chs3p on assembly of septins since the quantitative analysis of septin distribution indicates that it is very similar to that observed in the single *cdc10-11* mutant. However, we cannot rule out a possible interference of the absence of the chitin ring in septin function not detectable by our microscopic analysis. Growth at higher temperatures failed to provide additional clues since septin-deficient phenotypes were dominant, thus masking the role of other proteins. In terms of morphology and neck diameters, both double mutants differed, *cdc10-11* Δ*bni4* always showing more aberrant phenotypes and a greater enlargement of the neck diameter than *cdc10-11* Δ*chs3*, which again demonstrates that Bni4p exerts additional functions in septum assembly.

In conclusion, our results suggest new alternatives in the assembly of the septum and support genetic strategies that could be very useful in the determination of the function of other proteins involved in the process, including the role of transglycosidic linkages in septum formation.

ACKNOWLEDGEMENTS

We thank M. H. Valdivieso and E. Cabib for critical comments on the manuscript, and N. Skinner for language revision. We also thank Dr Rodríguez-Medina and Dr Cabib for plasmids and strains, and C. Belinchon and Dr Juan Fernandez for their help in electron microscopy. This work has been supported by a MEC predoctoral fellowship to M. S. Financial support came from CYCIT grant BIO2001-2048 and UE Grant QLK3-CT-2000-01537 to C. R.

REFERENCES

Baladron, V., Ufano, S., Duenas, E., Martin-Cuadrado, A. B., del Rey, F. & Vazquez de Aldana, C. R. (2002). Eng1p, an endo-1,3-beta-glucanase localized at the daughter side of the septum, is involved in cell separation in *Saccharomyces cerevisiae*. *Eukaryot Cell* **1**, 774–786.

Bi, E. (2001). Cytokinesis in budding yeast: the relationship between actomyosin ring function and septum formation. *Cell Struct Funct* **26**, 529–537.

Cabib, E. & Schmidt, M. (2003). Chitin synthase III activity, but not the chitin ring, is required for remedial septa formation in budding yeast. *FEMS Microbiol Lett* **29**, 299–305.

Cabib, E., Shaw, J. A., Mol, P. C., Bowers, B. & Choi, W. J. (1996). Chitin biosynthesis and morphogenetic processes. In *The Mycota. Biochemistry and Molecular Biology*, vol. III, pp. 243–267. Edited by R. Brambl & G. A. Marzluf. Berlin, Heidelberg: Springer.

Cabib, E., Roh, D. H., Schmidt, M., Crotti, L. B. & Varma, A. (2001). The yeast cell wall and septum as paradigms of cell growth and morphogenesis. *J Biol Chem* **276**, 19679–19682.

Choi, W. & Cabib, E. (1994). The use of divalent cations and pH for the determination of specific yeast chitin synthases. *Anal Biochem* **219**, 368–372.

Choi, W., Sburlati, A. & Cabib, E. (1994). Chitin synthase 3 from yeast has zymogenic properties that depend on both the *CAL1* and *CAL3* genes. *Proc Natl Acad Sci U S A* **91**, 4727–4730.

Cid, V. J., Duran, A., del Rey, F., Snyder, M. P., Nombela, C. & Sanchez, M. (1995). Molecular basis of cell integrity and morphogenesis in *Saccharomyces cerevisiae*. *Microbiol Rev* **59**, 345–386.

Cid, V. J., Adamikova, L., Cenamor, R., Molina, M., Sanchez, M. & Nombela, C. (1998). Cell integrity and morphogenesis in a budding yeast septin mutant. *Microbiology* **144**, 3463–3474.

Colman-Lerner, A., Chin, T. E. & Brent, R. (2001). Yeast Cbk1 and Mob2 activate daughter-specific genetic programs to induce asymmetric cell fates. *Cell* **107**, 739–750.

DeMarini, D. J., Adams, A. E. M., Fares, H., De Virgilio, C., Valle, G., Chuang, J. S. & Pringle, J. R. (1997). A septin-based hierarchy of proteins required for localized deposition of chitin in the *Saccharomyces cerevisiae* cell wall. *J Cell Biol* **139**, 75–93.

Fernandez-Abalos, J. M., Fox, H., Pitt, C., Wells, B. & Doonan, J. H. (1998). Plant-adapted green fluorescent protein is a versatile vital reporter for gene expression, protein localization and mitosis in the filamentous fungus, *Aspergillus nidulans*. *Mol Microbiol* **27**, 121–130.

Garcia-Rodriguez, L. J., Duran, A. & Roncero, C. (2000a). Calcofluor antifungal action depends on chitin and a functional high-osmolarity glycerol response (HOG) pathway: evidence for a physiological role of the *Saccharomyces cerevisiae* HOG pathway under noninducing conditions. *J Bacteriol* **182**, 2428–2437.

Garcia-Rodriguez, L. J., Trilla, J. A., Castro, C., Valdivieso, A., Duran, A. & Roncero, C. (2000b). Characterization of the chitin biosynthesis process as a compensatory mechanism in the *fks1* mutant of *Saccharomyces cerevisiae*. *FEBS Lett* **478**, 84–88.

Kaiser, C. A., Gimeno, R. E. & Shaywitz, D. A. (1997). Proteins secretion, membrane biogenesis, and endocytosis. In *The Molecular and Cellular Biology of the Yeast Saccharomyces*, vol. III, pp. 91–228. Edited by E. W. Jones, J. R. Pringle, & J. R. Broach. Cold Spring Harbor, NY: Cold Spring Harbor Laboratory.

Kollar, R., Petrakova, E., Ashwell, G., Robbins, P. W. & Cabib, E. (1995). Architecture of the yeast cell wall. The linkage between chitin and beta(1→3)-glucan. *J Biol Chem* **270**, 1170–1178.

Kozubowski, L., Panek, H., Rosenthal, A., Bloecher, A., DeMarini, D. J. & Tatchell, K. (2003). A Bni4-Glc7 phosphatase complex that recruits chitin synthase to the site of bud emergence. *Mol Biol Cell* **14**, 26–39.

Lippincott, J. & Li, R. (1998). Sequential assembly of myosin II, and IQGAP-like protein, and filamentous actin to a ring structure involved in budding yeast cytokinesis. *J Cell Biol* **140**, 355–366.

Longtine, M. S. & Bi, E. (2003). Regulation of septin organization and function in yeast. *Trends Cell Biol* **13**, 403–409.

Molano, J., Bowers, B. & Cabib, E. (1980). Distribution of chitin in the yeast cell wall: an ultrastructural and chemical study. *J Biol Chem* **85**, 199–212.

Ono, N., Yabe, T., Sudoh, M., Nakajima, T., Yamada-Okabe, T., Arisawa, M. & Yamada-Okabe, H. (2000). The yeast Chs4p protein stimulates the trypsin-sensitive activity of chitin synthase 3 through an apparent protein–protein interaction. *Microbiology* **146**, 385–391.

Orlean, P. (1997). Biogenesis of yeast wall and surface components. In *The Molecular and Cellular Biology of the Yeast Saccharomyces*, vol. III, pp. 229–362. Edited by E. W. Jones, J. R. Pringle, & J. R. Broach. Cold Spring Harbor, NY: Cold Spring Harbor Laboratory.

Rodriguez-Pena, J. M., Cid, V. J., Arroyo, J. & Nombela, C. (2000). A novel family of cell wall-related proteins regulated differently during the yeast life cycle. *Mol Cell Biol* **20**, 3245–3255.

Rodriguez-Pena, J. M., Rodriguez, C., Alvarez, A., Nombela, C. & Arroyo, J. (2002). Mechanisms for targeting of the *Saccharomyces cerevisiae* GPI-anchored cell wall protein Crh2p to polarised growth sites. *J Cell Sci* **115**, 2549–2558.

Roh, D. H., Bowers, B., Schmidt, M. & Cabib, E. (2002). The septation apparatus, an autonomous system in budding yeast. *Mol Biol Cell* **13**, 2747–2759.

Roncero, C. (2002). The genetic complexity of chitin synthesis in fungi. *Curr Genet* **41**, 367–378.

Roncero, C. & Duran, A. (1985). Effect of Calcofluor white and Congo red on fungal wall morphogenesis: in vivo activation of chitin polymerization. *J Bacteriol* **163**, 1180–1185.

Rose, M., Novick, P., Thomas, J., Bostein, D. & Fink, G. (1987). A *Saccharomyces cerevisiae* genomic plasmid bank based on a centromere-containing shuttle vector. *Gene* **60**, 237–243.

Rose, M. D., Winston, F. & Hieter, P. (1990). *Methods in Yeast Genetics: a Laboratory Course Manual*. Cold Spring Harbor, NY: Cold Spring Harbor Laboratory.

Rothstein, R. J. (1983). One-step gene disruption in yeast. *Methods Enzymol* **101**, 202–211.

Sambrook, J., Fritsch, E. F. & Maniatis, T. (1989). *Molecular Cloning: a Laboratory Manual*, 2nd edn. Cold Spring Harbor, NY: Cold Spring Harbor Laboratory.

Santos, B. & Snyder, M. (1997). Targeting of chitin synthase 3 to polarized growth sites in yeast requires Chs5p and Myo2p. *J Cell Biol* **136**, 95–110.

Sanz, M., Trilla, J. A., Duran, A. & Roncero, C. (2002). Control of chitin synthesis through Shc1p, a functional homologue of Chs4p specifically induced during sporulation. *Mol Microbiol* **43**, 1183–1195.

Schmidt, M., Bowers, B., Varma, A., Roh, D. H. & Cabib, E. (2002). In budding yeast, contraction of the actomyosin ring and formation of the primary septum at cytokinesis depend on each other. *J Cell Sci* **115**, 293–302.

Schmidt, M., Varma, A., Drgon, T., Bowers, B. & Cabib, E. (2003). Septins, under Cla4p regulation, and the chitin ring are required for neck integrity in budding yeast. *Mol Biol Cell* **14**, 2128–2141.

Shaw, J. A., Mol, P. C., Bowers, B., Silverman, S. J., Valdivieso, M. H., Duran, A. & Cabib, E. (1991). The function of chitin synthases 2 and 3 in the *Saccharomyces cerevisiae* cell cycle. *J Cell Biol* **114**, 111–123.

Tolliday, N., Pitcher, M. & Li, R. (2003). Direct evidence for a critical role of myosin II in budding yeast cytokinesis and the evolvability of new cytokinetic mechanisms in the absence of myosin II. *Mol Biol Cell* **14**, 798–809.

Tong, A. H., Lesage, G., Bader, G. D. & 47 other authors (2004). Global mapping of the yeast genetic interaction network. *Science* **303**, 808–813.

Trilla, J. A., Cos, T., Duran, A. & Roncero, C. (1997). Characterisation of *CHS4* (*CAL2*), a gene of *Saccharomyces cerevisiae* involved in chitin biosynthesis and allelic to *SKT5* and *CSD4*. *Yeast* **13**, 795–807.

Wang, H., Tang, X., Liu, J., Trautmann, S., Balasundaram, D., McCollum, D. & Balasubramanian, M. K. (2002). The multiprotein exocyst complex is essential for cell separation in *Schizosaccharomyces pombe*. *Mol Biol Cell* **13**, 515–529.